Ab initio simulation of ammonia monohydrate ($NH_3 \cdot H_2O$) and ammonium hydroxide (NH_4OH)

A. D. Fortes,[a] J. P. Brodholt, I. G. Wood, and L. Vočadlo,
Research School of Geological and Geophysical Sciences, Birkbeck College and University College London, Gower Street, London WC1E 6BT, United Kingdom

H. D. B. Jenkins
Department of Chemistry, University of Warwick, Coventry CV4 7AL, West Midlands, United Kingdom

(Received 11 June 2001; accepted 10 July 2001)

We report the results of the first pseudopotential plane-wave simulations of the static properties of ammonia monohydrate phase I (AMH I) and ammonium hydroxide. Our calculated fourth-order logarithmic equation of state, at zero pressure and temperature, has molar volume, $V_0 = 36.38(3)\ \mathrm{cm^3\,mol^{-1}}$, bulk modulus, $K_0 = 9.59(9)$ GPa, and the first derivative of the bulk modulus with respect to pressure, $K_0' = 5.73(21)$. Both this and the lattice parameters are in very good agreement with experimental values. The monohydrate transforms, via a solid-state proton transfer reaction, to ammonium hydroxide (NH_4OH) at 5.0(4) GPa. The equation of state of ammonium hydroxide is, $V_0 = 31.82(5)\ \mathrm{cm^3\,mol^{-1}}$, $K_0 = 14.78(62)$ GPa, $K_0' = 2.69(48)$. We calculate the reaction enthalpy, $\Delta H(\mathrm{NH_4OH}, s \rightarrow \mathrm{NH_3 \cdot H_2O}, s) = -14.8(5)\ \mathrm{kJ\,mol^{-1}}$ at absolute zero, and thus estimate the enthalpy of formation, $\Delta_f H^{\ominus}(\mathrm{NH_4OH}, s) = -356\ \mathrm{kJ\,mol^{-1}}$ at 298 K. This result places an upper limit of 84 $\mathrm{kJ\,mol^{-1}}$ on the barrier to rotation of the ammonium cation, and yields an average hydrogen bond enthalpy of $\sim$23 $\mathrm{kJ\,mol^{-1}}$. © *2001 American Institute of Physics.* [DOI: 10.1063/1.1398104]

I. INTRODUCTION

The stoichiometric hydrates of ammonia are of great theoretical and physical significance. This system is the simplest to contain mixed (hetero- and homonuclear) hydrogen bonds of the kind common in many biomolecules, and the polymorphs identified to date exhibit a rich diversity of hydrogen bond geometries.[1] The potential for proton transfer under compression has also been mooted,[2] and this is another process of biological importance. Hence, the behavior of the hydrogen bonds in AMH may exhibit properties which are transferable to much more complex molecular solids.

Ammonia hydrates are also very likely to comprise an important fraction of the condensed volatile mineral (CVM) component of icy moons orbiting Saturn, Uranus and Neptune. Planetary accretion models[3] and photogeologic observations of cryovolcanic landforms,[4] combined with isotopic studies of Titan's volatile reservoir,[5] strongly indicate that the CVM component contains $\sim 5-15$ wt% NH_3. The ambient pressure phase diagram[4] reveals, therefore, that ammonia dihydrate (ADH) will be a major mineral species in icy moons. Small density contrasts between the solid and liquid phases,[6] and the weak gravity fields associated with small low-density satellites, militate against fractional crystallization. It is thus unlikely that compositions on the ammonia-rich side of the eutectic (32 wt% NH_3 at 100 kPa) occur naturally in icy satellites. However, ADH is known to decompose into ammonia monohydrate + ice VII at pressures of around 3.5 GPa.[7] It is therefore plausible that the monohydrate phase was present in the cold (100–130 K), mixed ice-rock core of post-accretion Titan, wherein peak pressures may have just exceeded 4 GPa, and it has been proposed that ammonia monohydrate played a major role in the evolution of Titan's core.[8]

We are interested, therefore, in understanding the phase relations and physical characteristics of polymorphs across the whole ammonia-water system. As part of a broader ongoing study into solids in the ammonia-water system,[9,10] we present here the results of our initial investigation of $NH_3 \cdot H_2O$. In Sec. II we commence with a brief description of the structure and phase relations thus far experimentally established in the AMH system. This is followed in Sec. III by an account of the computational method employed in the simulation of AMH I and ammonium hydroxide, and Sec. IV reports our results. The results are divided into three subsections. The first describes the fitting of an equation of state (EOS) to the energy-volume curves and compares our results with recent experimental data. The second subsection deals with the structures of AMH I and ammonium hydroxide, and describes the variation of a number of internal parameters as a function of pressure. The third subsection deals with the thermodynamics of the two phases. We end with a short summary and discussion of the implications of our results for the other stoichiometric solids in the ammonia-water system.

II. STRUCTURE AND PHASE RELATIONS

Ammonia monohydrate is orthorhombic, space group $P2_12_12_1(D_2^4)$, at ambient pressure (AMH phase I), and con-

[a]Author to whom correspondence should be addressed. Electronic mail: ucfbanf@ucl.ac.uk

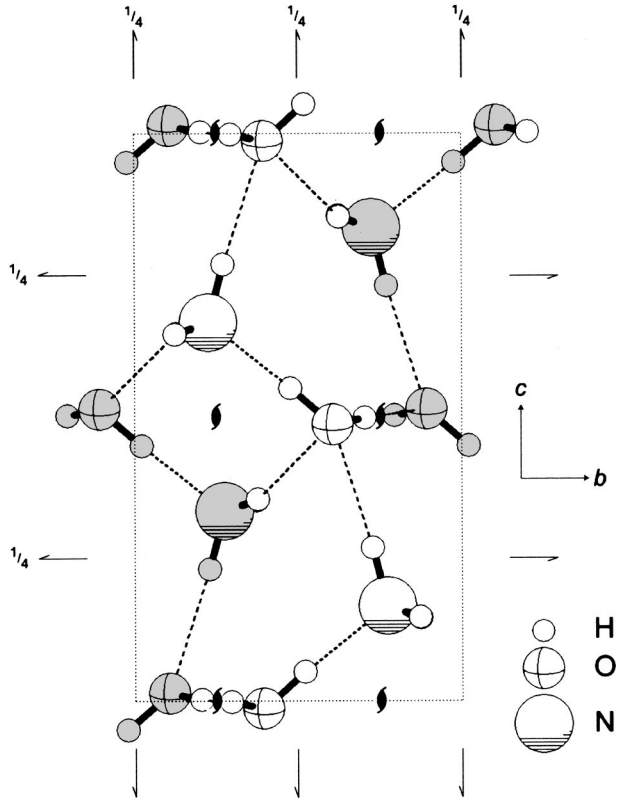

FIG. 1. The ambient pressure structure of ammonia monohydrate phase I (AMH I) (Ref. 1). Covalent O–H and N–H bonds are depicted as thick rods, and hydrogen bonds as dashed lines. Diad screw axes are indicated by the symbol.

tains four molecules per unit cell.[1] The structure (Fig. 1) is fully proton ordered, consisting of moderately strongly hydrogen-bonded chains of water molecules, extending along the *a*-axis, cross-linked by weakly hydrogen-bonded ammonia molecules. Each ammonia molecule is tetrahedrally coordinated by four water molecules, donating three weak *h*-bonds, and accepting a single stronger *h*-bond. Each water molecule is 6-coordinated, bonding to four ammonia molecules and two other water molecules. Lattice parameters and internal coordinates are given in Table I. The fractional coordinates in Table I are the starting point for our structural relaxations, as described in the following section.

At temperatures above 130 K, AMH I transforms to another orthorhombic structure (AMH II) with a cell volume of $\sim 750\ \text{Å}^3 (Z=16)$ at ~ 0.5 GPa, and subsequently to another structure (AMH IV) at 2.2 GPa,[11] as shown in Fig. 2. Below 130 K, the transformation to AMH II appears to be suppressed, such that AMH I transforms directly to AMH IV. Diffraction patterns of AMH IV have been indexed with a monoclinic unit cell [$a=11.198(6)$ Å, $b=6.843(6)$ Å, $c=5.284(11)$ Å, $\beta=105.65(3)°$ at 4.2 GPa, and 180 K] containing nine formula units.[8] The detailed molecular structure of AMH IV and the sequence of phase transformations below 130 K, and at pressures >7 GPa, are presently unknown.

III. COMPUTATIONAL METHODS

The combination of relatively high symmetry, small unit cell and orientational order of the water and ammonia molecules makes AMH I an ideal material with which to begin simulating the behavior of mixed solids in the ammonia-water system.

Ammonia monohydrate was first simulated by Brink and Glasser[12] using the empirical interatomic potential function EPEN/2. Their relaxed structure matched experimental data quite well, yielding a lattice energy of 86.02 kJ mol^{-1}. However, the use of empirical potential functions is clearly less satisfactory than a fully quantum mechanical treatment, such as we employ here.

The *ab initio* pseudopotential method, based on density functional theory,[13] was used for calculating the total energy of the crystal lattice. The Perdew–Wang generalized gradient corrected functional (PW91) was used to represent the exchange-correlation potential,[14] this form of the generalized gradient approximation (GGA) having been demonstrated to yield the most accurate results in hydrogen-bonded systems.[15,16] Core electrons are replaced by Vanderbilt nonnormconserving ultrasoft pseudopotentials,[17] themselves formulated within the GGA, and the valence electron wave functions are expanded as a plane-wave basis set. Total energy calculations were performed using the VASP (Vienna *ab initio* simulation package) code.[18] Total energy convergence tests were carried out to optimize the sampling of the Brillouin zone, and the cutoff of the plane-wave basis set; the Monkhorst–Pack scheme[19] was used for sampling of the Brillouin zone. It was found that a grid with 32 symmetrically unique $\vec{k}$-points in the irreducible wedge, combined with a kinetic energy cutoff of 1100 eV, yielded total energy convergence to better than 10^{-4} eV per unit cell. A series of fixed volume calculations were then performed in which the ions were allowed to move. For each volume specified, the structure was relaxed in order to optimize the lattice parameters and internal coordinates.

As a test of the reliability of the supplied pseudopotentials, we calculated the relaxed geometry of isolated monomers of both water and ammonia. For the isolated water molecule we found the O–H bond length, $r_{(\text{O–H})}=0.970$ Å, and the bond angle, H–$\hat{\text{O}}$–H$=104.74°$. These compare well with the experimental values of 0.957 Å and 104.52°.[20] For the isolated ammonia molecule we found the N–H bond length, $r_{(\text{N–H})}=1.022$ Å, and the bond angle H–$\hat{\text{N}}$–H $=107.29°$. Again, these are a good match to the experimental values, 1.011 Å and 106.80°.[21] The error of 1–1.5% in the length of the X–H bond is largely due to inadequacies in the hydrogen pseudopotential. In principle, this can be corrected by a slight increase in the strength of the nonlocal part of the pseudopotential.[22]

Our simulated lattice is hydrogenous, but differences from the experimental structure, which is deuterated, are likely to be minor. In neutral water clusters, hydrogen bonds are ~ 0.8 kJ mol^{-1} weaker than deuteron bonds, although this situation is reversed in charged clusters.[23] Hence, hydrogenous AMH will be marginally more weakly bound than its deuterated counterpart, and the opposite will be true for ammonium hydroxide. The difference is due to the zero-point vibrational motion associated with one of the intermolecular wagging modes.[23] A further result is that the O–$\hat{\text{H}}$...O angle

TABLE I. Zero pressure structural parameters of AMH I from experiment and calculation. All atoms are sited on Wykoff positions $4a$ within space group $P2_12_12_1$.

	Experimental values[a]			Calculated values[b]		
a (Å)	4.51108(14)			4.49505		
b (Å)	5.58691(20)			5.54476		
c (Å)	9.71452(34)			9.70787		
b/a	1.2385(1)			1.2335		
c/a	2.1535(1)			2.1597		
V (Å^3)	244.835(25)			241.959		
Fractional atomic coordinates						
	x	y	z	x	y	z
O1	0.2475(12)	0.1065(5)	0.0136(3)	0.2654	0.1141	0.0246
H1	0.4348(7)	0.2047(5)	0.0021(5)	0.4472	0.2136	0.0059
H2	0.2422(14)	0.0219(4)	0.4490(3)	0.2346	0.0210	0.4520
N1	0.2437(9)	0.2740(3)	0.3336(2)	0.2418	0.2547	0.3413
H3	0.4172(15)	0.3758(9)	0.3542(6)	0.4253	0.3588	0.3616
H4	0.0713(15)	0.3731(9)	0.3530(6)	0.0603	0.3626	0.3578
H5	0.2378(11)	0.2287(5)	0.2313(2)	0.2455	0.2084	0.2390
Bond lengths (Å)						
O1–H1	1.013(5)			1.003		
O1–H2	0.955(3)			1.029		
H1...O1	1.768(5)			1.745		
O1...O1	2.780(3)			2.748		
N1–H3	0.988(6)			1.026		
N1–H4	0.973(6)			1.024		
N1–H5	1.025(3)			1.026		
H3...O1	2.367(7)			2.271		
H4...O1	2.335(7)			2.322		
H5...O1	2.223(4)			2.148		
H2...N1	1.800(3)			1.683		
Bond angles						
O1–H1...O1	175.95(37)°			179.29°		
O1–H2...O1	175.99(29)°			176.24°		
N1–H3...O1	158.43(50)°			159.46°		
N1–H4...O1	153.61(55)°			158.38°		
N1–H5...O1	175.55(21)°			178.49°		

[a]Reference 1.
[b]This work.

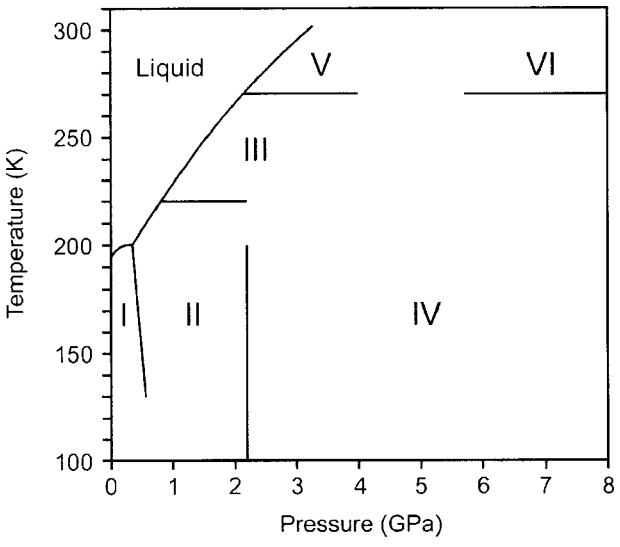

FIG. 2. Phase diagram of ammonia monohydrate (Ref. 1).

will be smaller than the equivalent O–D̂...O angle in AMH. However, it is worth noting that deuteration is known to have very large effects in some hydrogen bonded systems.[24]

IV. RESULTS

A. Equation of state

Structural relaxations were carried out at fixed cell volumes from 42.15 cm^3 mol^{-1} (280 Å^3) to 18.07 cm^3 mol^{-1} (120 Å^3). These revealed a discontinuity at ~27.1 cm^3 mol^{-1} (180 Å^3) in the slope of the total energy curve (Fig. 3), the pressure (Fig. 4), and the lattice parameters (Fig. 5), indicative of a first-order phase transition. Examination of the fractional atomic coordinates showed that the molecular AMH I structure had become an ionic solid, transforming via a solid-state protolytic reaction to ammonium hydroxide (NH_4OH). This is the first time that this structure has been observed. Subsequently, we were able to relax the ionic structure at volumes within the field of stability of AMH I. An integrated form of the third-order Birch–Murnaghan equation of state

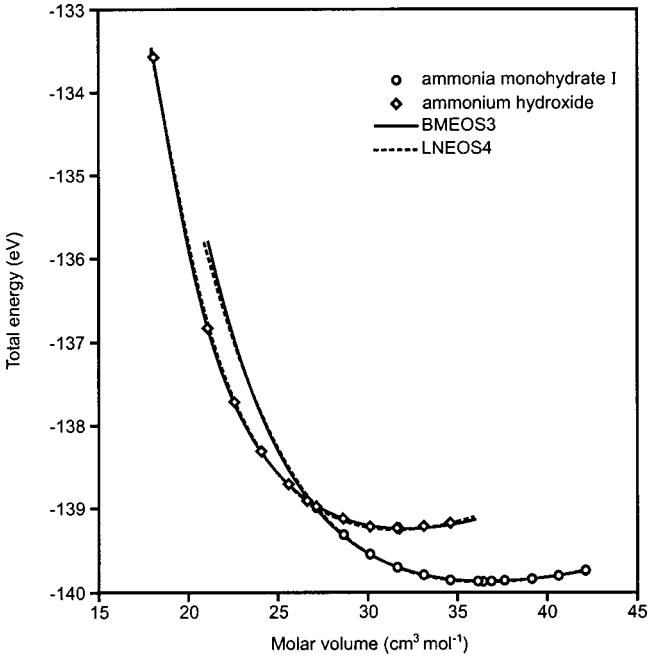

FIG. 3. $E(V)$ curves for AMH I and ammonium hydroxide. Full and dashed lines represent fitted third-order Birch–Murnaghan and fourth-order logarithmic equations of state respectively. Equation of state parameters are reported in Table II.

(BMEOS3),[25] and of the fourth order logarithmic equation of state (LNEOS4)[26] were fitted to the energy-volume data for the molecular and ionic phases (Fig. 3). It is noteworthy that the BMEOS and LNEOS fits to the ammonium hydroxide calculation differ somewhat. However, the LNEOS fit is superior in that part of the $E(V)$ curve close to the zero pressure volume, V_0, as evidenced by the slightly improved correlation coefficient shown in Table II.

The equations of state (EOS) of AMH I and AMH IV were measured recently[8] and we find the calculated EOS of

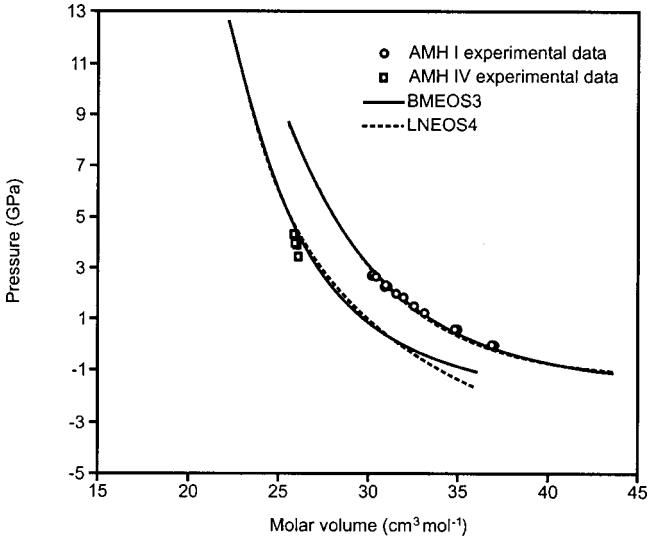

FIG. 4. Comparison of the calculated equations of state of AMH I and ammonium hydroxide with the measured equations of state of AMH I and AMH IV (Ref. 8). Data for AMH I was collected at 115, 130, and 150 K. Equation of state parameters are reported in Table II.

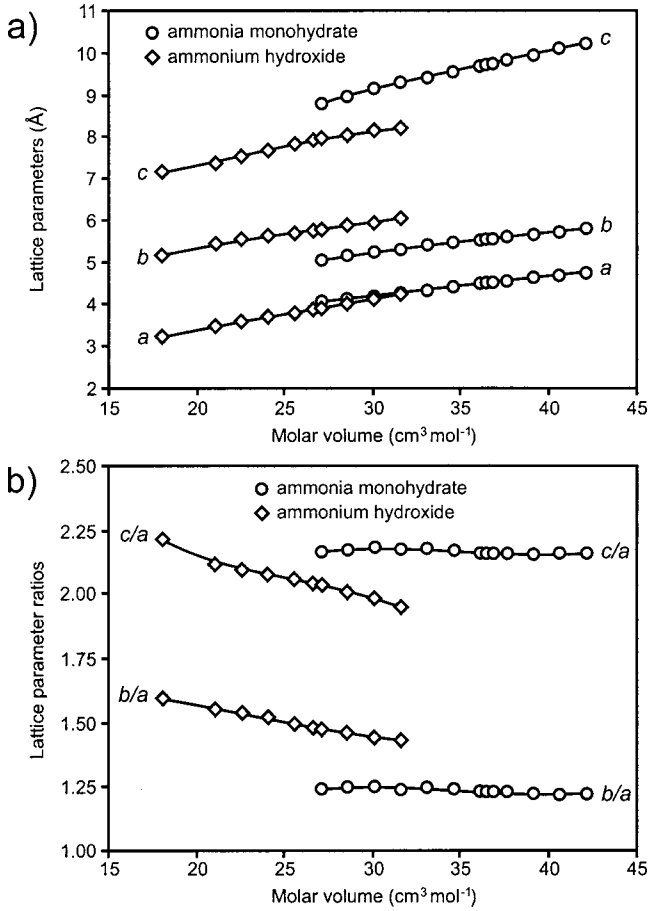

FIG. 5. Variation in, (a) lattice parameters, and (b) lattice parameter ratios as a function of molar volume.

AMH I compares very well with the experimental data points in Fig. 4. We have fitted a Murnaghan integrated linear equation of state[27] and a third-order Birch–Murnaghan equation of state[25] (MILEOS and BMEOS3) to the experimental data points so as to afford a more quantitative comparison with our results. These are reported in Table II. We also fitted a second-order BMEOS and the U2 and U3 ''universal'' equations of state[28,29] to the experimental data, but the results do not differ substantially from the tabulated fits. The calculated zero pressure volume of AMH I is in excellent agreement with the measured ambient pressure volume [36.860(4) $cm^3\,mol^{-1}$ at 110 K]. We have found in practice[9,10] that the PW91 GGA functional compensates extremely well for the known deficiencies of the local density approximation (LDA),[30] such as over-binding, in glacial solids of water and ammonia. Indeed the thermal expansion coefficient derived by Croft *et al.*[31] provides us with a value for V_0 at zero Kelvin of 36.552(3) $cm^3\,mol^{-1}$, and this differs by just 0.3% from our calculated value. Our bulk modulus, K_0, is marginally stiffer than the experimental data suggest, and this may be due to inadequacies in the description of core-valence exchange-correlation energy within the GGA pseudopotentials.[32]

Although there are no experimental values of V_0 for ammonium hydroxide, we may gauge the accuracy of our calculations by reference to published volumetric data[33] for the

TABLE II. Calculated equations of state of AMH I and ammonium hydroxide, compared with analytical fits to graphical data in Ref. 8. Coefficients of multiple determination (R^2) are included to indicate the quality of fit. Errors are those resulting from the fitting procedure; the true errors will be larger.

	Molecular AMH I[a]		Molecular AMH I[b]			Ionic ammonium hydroxide[a]	
	BMEOS3	LNEOS4	MILEOS	BMEOS3	LNEOS4	BMEOS3	LNEOS4
V_0 ($cm^3\,mol^{-1}$)	36.417(13)	36.384(27)	37.135(25)	37.03(12)	37.05(14)	31.872(115)	31.824(53)
K_0 (GPa)	9.55(6)	9.59(9)	8.81(8)	9.40(62)	9(2)	11.93(58)	14.78(62)
K_0'	5.44(8)	5.73(21)	3.93(4)	3.61(49)	5(5)	6.21(19)	2.69(48)
K_0'' (GPa^{-1})	⋯	−1.24(46)	⋯	⋯	−0.29(87)	⋯	1.59(11)
E_0 (eV $atom^{-1}$)	−4.9954(1)	−4.9954(1)	⋯	⋯	⋯	−4.9727(1)	−4.9730(1)
R^2 (%)	99.9981	99.9984	99.9934	99.7809	99.7620	99.9974	99.9992

[a]This work.
[b]Fits to data in Ref. 8.

ions concerned, as is common practice for estimating the molar volumes of salts. The thermochemical volume for the NH_4^+ ion is given as $0.021 \pm 0.015\,nm^3$, and that of the OH^- ion as $0.032 \pm 0.008\,nm^3$. These values yield a molar volume for NH_4OH of $31.92 \pm 13.85\,cm^3\,mol^{-1}$, which is in close agreement with our calculated value (Table II). A further constraint may be applied using the volume of the hydration water in ammonium hydroxide. The proposed value[34] of $13.0 \pm 2.1\,cm^3\,mol^{-1}$, added to the molar volume of solid ammonia at zero Kelvin,[35] $19.37\,cm^3\,mol^{-1}$, gives V_0 for $NH_4OH = 32.37 \pm 2.1\,cm^3\,mol^{-1}$.

We now compare the calculated and experimental structures and describe the behavior of simulated AMH I and ammonium hydroxide under compression.

B. Structures

A comparison of the experimental and simulated lattice parameters, internal coordinates, bond lengths, and bond angles of AMH I at zero pressure (Table I) shows close agreement. The cell volume dependence of the lattice parameters is presented in Figs. 5(a) and 5(b).

The greatest difference between the observed and calculated bond lengths (Table I) is for the covalent O–H and N–H bonds. This discrepancy arises from the hydrogen pseudopotential, as described in Sec. III. What is puzzling about the experimental structure is that the large variation in N–H bond lengths should appear as a difference of several hundred wave numbers in the N-D stretching frequency, ν_{N-D}. Published spectroscopic data[36] do not support this, ν_{N-D} being quoted as 2464.1, 2467.0, and 2471.3 cm^{-1}. Our N–H bond lengths are tightly clustered around 1.025 Å while the experimental values range from 0.973 Å to 1.025 Å. Large differences between O–H1 and O–H2 are endorsed by the published O-D stretching frequencies:[36] $\nu_{O-D} = 2410$ and 2197 cm^{-1}. The difference in length between our O–H bonds (0.032 Å) is similar to the experimental value (0.058 Å).

The behavior of the hydrogen bond strength under pressure in AMH is of some interest and has yet to be studied experimentally. In both ice and ammonia, the hydrogen bond is pressure strengthened, leading to an increase of $r_{(O-H)}$ or $r_{(N-H)}$. In water ice this continues up to the limit in which the proton is symmetrically located halfway between the heavy atoms, producing the Cu_2O isomorph dubbed ice X. However, we found[10] that our calculated pressure dependence of the O–H bond length in ice VIII is overestimated by a factor of ~2 up to 20 GPa when compared with experimental data[37] and *ab initio* Hartree–Fock studies.[37,38] Nevertheless, the correct overall behavior is reported, and the transition pressure from ice VIII to ice X is in agreement with experimental observations.

Our best estimate[10] of $\partial r_{(O-H)}/\partial P$ in ice VIII, up to 10 GPa, is 0.11(1) pm GPa^{-1}. In AMH, however, up to 5 GPa, we find that $r_{(O-H1)}$ increases at 0.27(2) pm GPa^{-1}, and $r_{(O-H2)}$ increases at 0.85(1) pm GPa^{-1} (Fig. 6). By contrast, the N–H bond length remains constant (i.e., $\partial r/\partial P = 0$) at all pressures up to 5 GPa: $r_{(N-H3)} = 1.026(1)$ Å, $r_{(N-H4)} = 1.023(1)$ Å, and $r_{(N-H5)} = 1.025(1)$ Å. Once again, this differs from our work on solid ammonia[33] in which $r_{(N-H)}$ increased by 0.038(1) pm GPa^{-1} up to 4 GPa. Our preliminary results for ammonia hemihydrate reveal the same pressure dependence of hydrogen bond strength, leading to a similar protonation of the N1 atom.

A critical test of the simulation would be the direct measurement of the variation in interatomic distances as a function of pressure by neutron diffraction or by inference from spectroscopic data.

Note that the bond angles in Table I are all larger in the

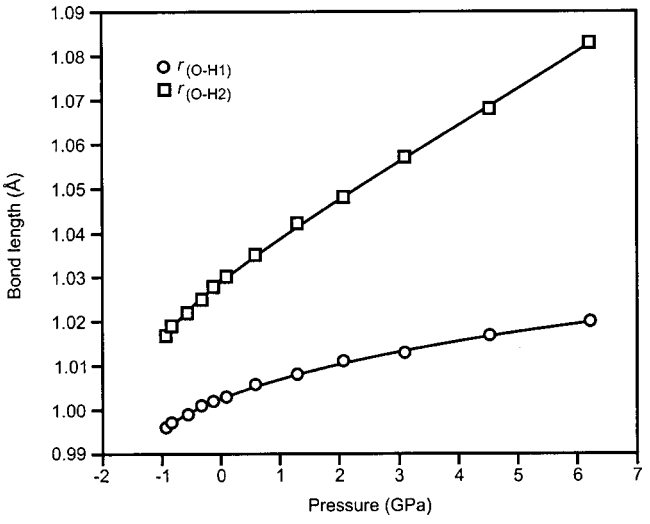

FIG. 6. Pressure dependence of $r_{(O-H1)}$ and $r_{(O-H2)}$ in AMH I.

TABLE III. Calculated structural parameters for ammonium hydroxide at ~5 GPa. All atoms are sited on Wykoff positions 4*a* within space group $P2_12_12_1$.

Cell Parameters			
a (Å)		3.80112	
b (Å)		5.70064	
c (Å)		7.84538	
b/*a*		1.4997	
c/*a*		2.0640	
V (Å^3)		170.000	
Fractional atomic coordinates			
	x	*y*	*z*
O1	0.11109	0.08134	0.98168
H1	0.28924	0.20608	0.98614
N1	0.37757	0.35231	0.33872
H2	0.35236	0.17760	0.37769
H3	0.58731	0.42664	0.40485
H4	0.16114	0.44800	0.37820
H5	0.43323	0.36829	0.20811
Bond lengths (Å)			
O1–H1		0.999	
H1...O1		1.736	
O1...O1		2.725	
N1–H2		1.057	
N1–H3		1.063	
N1–H4		1.046	
N1–H5		1.057	
H2...O1		1.690	
H3...O1		1.667	
H4...O1		1.746	
H5...O1		1.699	

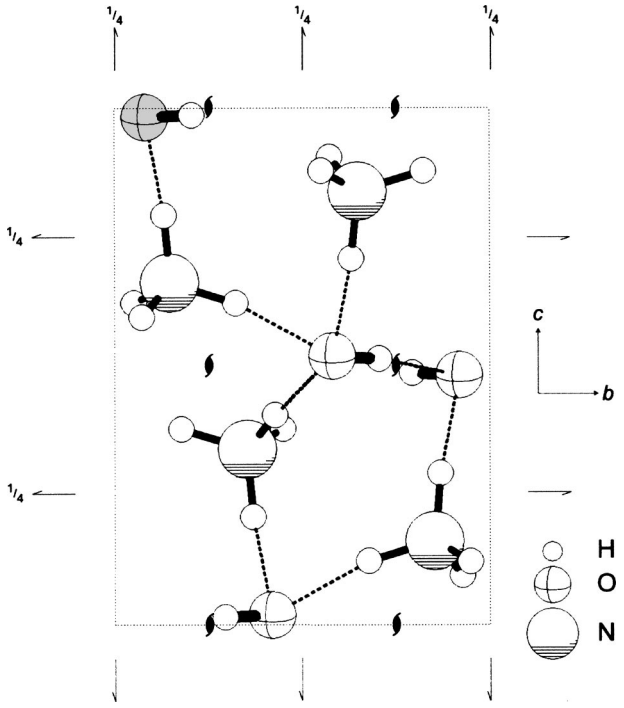

FIG. 7. The structure of ammonium hydroxide at ~5 GPa. Covalent O–H and N–H bonds are depicted as thick rods, and hydrogen bonds as dashed lines. Diad screw axes are indicated by the symbol.

hydrogenous calculated structure than in the deuterated experimental structure, as expected.[18]

In ammonium hydroxide, the variation in bond lengths changes once more. Within its field of stability, above 5 GPa, $r_{(O-H1)}$ increases at 0.05 pm GPa^{-1}. The N–H bond created upon the formation of ammonium hydroxide increases in length at a very much reduced rate: $\partial r_{(N-H2)}/\partial P = 0.005$ pm GPa^{-1}. The remaining N–H bonds all decrease in length at approximately the same rate, $-0.05(1)$ pm GPa^{-1}. An interesting feature, revealed in Table III, is the similarity of all of the hydrogen bond lengths in ammonium hydroxide. This represents a significant departure from the structure of AMH wherein the O–H...O, O–H...N, and N–H...O hydrogen bonds are all of greatly differing lengths, and is the result of the OH^- anion being a particularly strong hydrogen bond acceptor.[39]

Our determination of the equilibrium O–H bond length for the isolated hydroxide molecule is 0.984 Å, compared with the spectroscopically observed value of 0.96973 Å,[40] a difference of ~1.5%, which is in line with the overestimation of the X–H bond lengths of the free water and ammonia molecules reported in Sec. III.

We also performed calculations to determine the equilibrium geometry of the isolated ammonium monomer and found the N–H bond length, $r_{(N-H)} = 1.055$ Å, and the bond angle, $H–\hat{N}–H = 109.38°$. The bond angle is very close to what one would expect for a molecule with T^D symmetry, i.e., $H–\hat{N}–H = \arccos(-\frac{1}{3}) = 109.47°$. The equilibrium N–H bond length for the gas phase NH_4^+ ion has been measured spectroscopically, and has also been the subject of numerous *ab initio* simulations. The results yield a best estimate of $r_{(N-H)} = 1.0203$ Å.[21] Our value of $r_{(N-H)}$ exceeds this by over 3% however. It is not clear why the X–H bond length should be overestimated by so much more than for the other molecules we investigated.

We might expect that hydrogen bonding would tend to increase the length of X–H bonds in the solid state. However, in ammonium crystals, with the exception of NH_4F, the evidence for hydrogen bonding is very weak.[41] Even in NH_4F(I) and NH_4HF_2 the N–H bond lengths are increased to just 1.025(5) Å[42] and 1.030(2) Å,[43] respectively. In the higher density NH_4F(II), the N–H bonds are generally shorter than in NH_4F(I), although $r_{(N2-D5)} = 1.068(5)$ Å.[42] Whilst we will offer evidence in the ensuing subsection for the presence of hydrogen bonding, it appears to have little effect on the X–H bond lengths in ammonium hydroxide.

Figure 4 shows that there is an encouraging agreement between the equations of state of AMH IV and our simulated ionic phase. However, our ammonium hydroxide structure retains all of the symmetry elements of space group $P2_12_12_1$ (Fig. 7). Given that the atomic structure of AMH IV is presently unknown, we can confirm that the hydroxide is not AMH IV by simulating the neutron diffraction pattern of ND_4OD. Figures 8(a) and 8(b) show the measured and calculated patterns of deuterated AMH I, reassuring us that our simulated structure is indeed the same as that seen in the laboratory, and that our diffraction simulation package yields

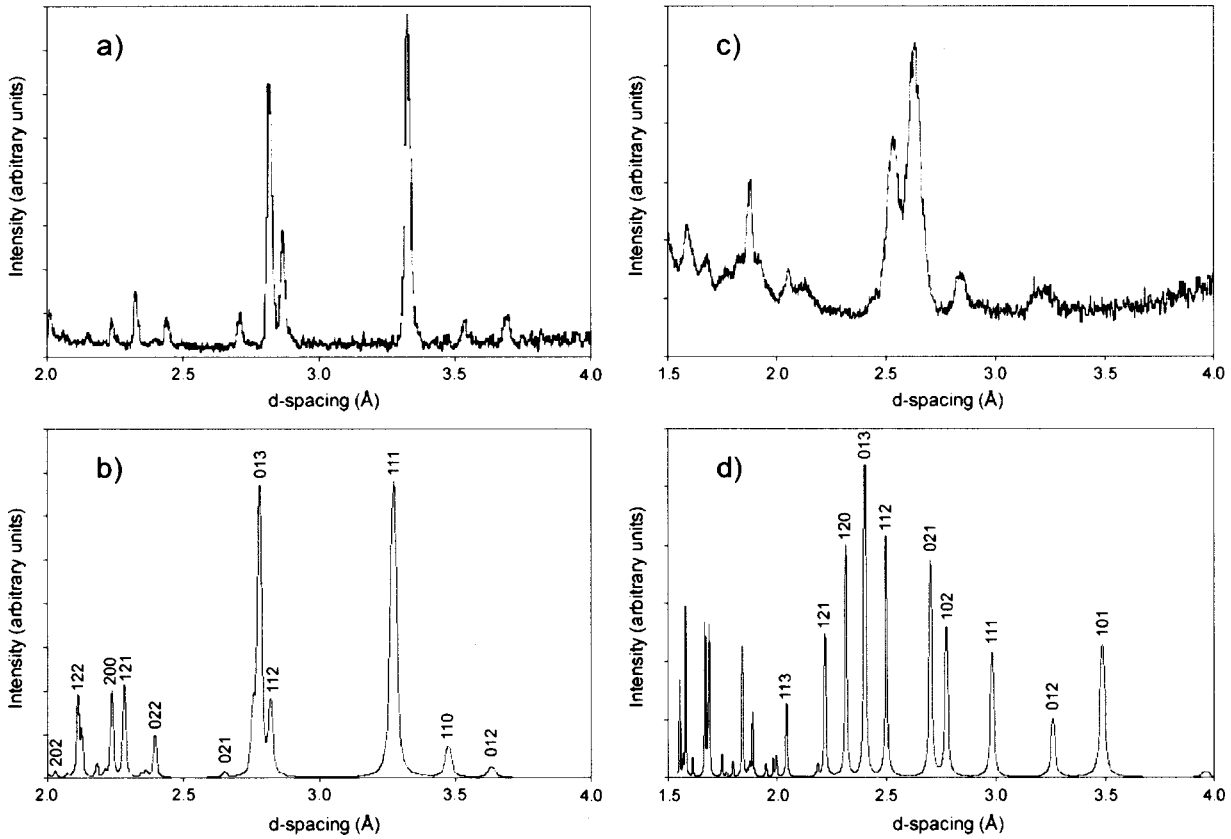

FIG. 8. (a) The measured neutron diffraction profile of AMH I at ambient pressure, 110 K (Ref. 9). (b) Calculated diffraction pattern of our AMH structure at ~800 bar. (c) The measured neutron diffraction profile of AMH IV at 3.7 GPa, 180 K (Ref. 9). (d) Calculated diffraction pattern of our NH_4OH structure at 3.74 GPa.

sensible results. Figures 8(c) and 8(d) show the measured pattern of deuterated AMH IV, and the calculated pattern of ND_4OD, respectively. Clearly, the two are very different. We conclude from this, therefore, that the protolysis reaction in AMH, at least above 130 K, is interrupted by a phase transformation to a denser molecular solid (AMH II or AMH IV). The similarity in the EOS of AMH IV and NH_4OH is thus coincidental. This does not rule out the existence of an ionic solid at lower temperatures, or at higher pressures, than have been studied experimentally to date.

In addition to structural parameters, our total energy calculations permit us to arrive at some thermodynamic quantities for the ammonium hydroxide via known thermodynamic properties of AMH I, and this is the subject of the following section.

C. Thermodynamics

The enthalpy (H) of the two phases (Fig. 9) is calculated from the respective equations of state ($H=U+PV$), yielding the transition pressure in the athermal limit as 5.0(4) GPa. The calculation of the enthalpy difference between the two phases can also be used to more closely constrain certain thermodynamic quantities that, for ammonium hydroxide, have previously only been estimated. The earliest estimate of the enthalpy of formation, $\Delta_f H^{\ominus}(NH_4OH,s)$, appears in Karapet'yants and Karapet'yants.[44] However, the value of $-326\ \mathrm{kJ\,mol^{-1}}$ does not appear in their referenced source. Johnson[2] surveyed the thermochemistry of known ammonium salts and used the results to determine the stability of ammonium hydroxide. The thermodynamic quantities quoted in Ref. 2 are $\Delta_f H^{\ominus}(NH_4OH,s)=-275\ \mathrm{kJ\,mol^{-1}}$, and $\Delta G(NH_3\cdot H_2O,s\rightarrow NH_4OH,s)=98\ \mathrm{kJ\,mol^{-1}}$, at 110 K, neglecting the entropy term, $T\Delta S$. Interpolation of the molar volumes of KOH and RbOH yielded an estimated molar volume of 28.40 $\mathrm{cm^3\,mol^{-1}}$ for NH_4OH. Combined with the estimated free energy change of the protolytic reaction, a transition pressure of ~12 GPa was forecast.

Our total energy calculations allow us to determine the

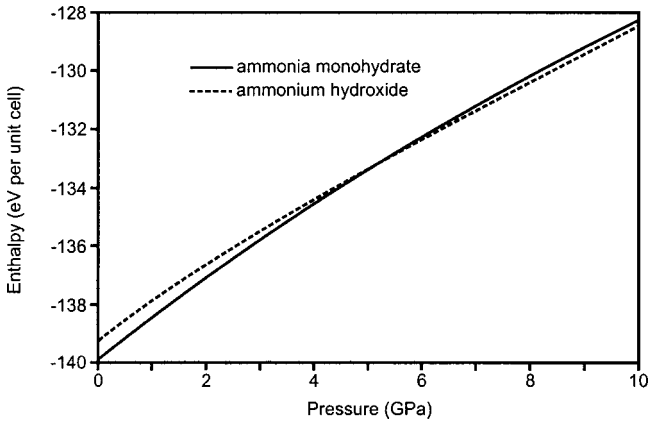

FIG. 9. Enthalpy of AMH and ammonium hydroxide.

relative enthalpy differences between ammonia monohydrate and ammonium hydroxide. Figure 9 reveals that the protolytic reaction occurs (i.e., the enthalpy change, $\Delta H=0$) at a pressure of ~5 GPa, and that the enthalpy difference between the two phases at zero pressure is 14.8(5) kJ mol^{-1}. This enthalpy change corresponds to that for the reaction $NH_3 \cdot H_2O,s \rightarrow NH_4OH,s$ at zero Kelvin. It is then straightforward to calculate $\Delta_f H^{\ominus}(NH_4OH,s)$ using existing thermodynamic data for the monohydrate phase. From Ref. 45, $\Delta_f H^{\ominus}(NH_3 \cdot H_2O,l) = -361.8$ kJ mol^{-1}. The change in enthalpy from 298 K to 0 K, $H^{\ominus}_{298} - H^{\ominus}_0$, is found from the measured heat capacity and added to the heat of fusion (6560.5 J mol^{-1})[46] to give $\Delta_f H^{\ominus}(NH_3 \cdot H_2O,s) = -391.8$ kJ mol^{-1} at zero Kelvin. Combining this with our calculated reaction enthalpy gives $\Delta_f H^{\ominus}(NH_4OH,s) = -376$ kJ mol^{-1}. We may now estimate the enthalpy of formation at 298 K by assuming that the heat capacities of the solid monohydrate and hydroxide are the same, yielding $\Delta_f H^{\ominus}(NH_4OH,s) = -356$ kJ mol^{-1}. There are two significant corollaries to this result.

The first arises from the difference between our results and those of Johnson,[2] and so it is necessary to evaluate the sources of error noted in the earlier work. Most important of all is the neglect of lattice stabilization due to lowered cation symmetry (SLCS):[2,4]

$$\mathrm{SLCS} \approx E_a = 142 - \frac{1}{n}\{\Delta_f H^{\ominus}[(NH_4)_n X,c] - \Delta_f H^{\ominus}(Rb_n X,c)\}\ \mathrm{kJ\,mol^{-1}}, \quad (1)$$

where E_a is the activation energy barrier to reorientation of the ammonium ion.

Johnson[2] predicted that the departure from sphericity of the NH_4^+ ion, and resulting cation-anion hydrogen bonding, should stabilize the lattice energy by ~50 kJ mol^{-1}. However, in estimating $\Delta_f H^{\ominus}(NH_4OH,s)$, a value of zero was assumed for SLCS. Applying the simple ionic model (Eq. 1), our value of $\Delta_f H^{\ominus} = -356$ kJ mol^{-1} gives a stabilization energy of ~84 kJ mol^{-1}, which is rather large but agrees with the expectation that ammonium hydroxide is very strongly hydrogen-bonded. Moreover, the ionic model allows us to predict that 84 kJ mol^{-1} is a likely upper limit for the energy barrier to cation reorientation (E_a) in solid ammonium hydroxide; by comparison with other materials in which the ammonium ion is strongly hydrogen-bonded (i.e., aqueous NH_4^+ and NH_4F), we can predict that the energy barrier is almost certainly much smaller, perhaps by as much as 50%.[46] This appears to be the result of a different rotation mechanism (carousel rotation of the NH_4^+ ion about the C_3 axis, as opposed to rotation about an S_4 axis) to that seen in other ammonium salts.[46,47] This mechanism, in which the axial N–H bond length in the transition state increases, has the implication that the ammonium ion might return its axial proton to the neighboring OH^- ion, reversing the protolysis to yield AMH.[47] The height of the energy barrier could be experimentally determined by nuclear magnetic resonance (NMR) spectroscopy.

The second major corollary to our calculation of the reaction enthalpy is the determination of the lattice potential energy (U_{POT}), and the enthalpy of solution ($\Delta_{soln}H^{\ominus}$), of ammonium hydroxide. There are two ways to find U_{POT}. First, one can construct a conventional Born–Fajans–Haber cycle (Fig. 10) using the known enthalpy of formation of the salt in question or, second, one can use a volume-based empirical formula to calculate the lattice enthalpy.

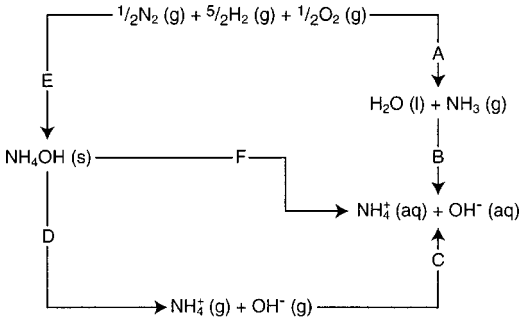

FIG. 10. Born–Fajans–Haber cycle for NH^{4}OH. Path $A = \Delta_f H^{\ominus}(H_2O,l) + \Delta_f H^{\ominus}(NH_3,g)$; path $B = \Delta_{soln}H^{\ominus}(NH_3,g)$; path $C = \Delta_{hyd}H^{\ominus}(NH_4^+,g) + \Delta_{hyd}H^{\ominus}(OH^-,g)$; path $D = \Delta_L H^{\ominus}(NH_4OH,s) = U_{pot} + \frac{3}{2}RT$; path $E = \Delta_f H^{\ominus}(NH_4OH,s)$; and path $F = \Delta_{soln}H^{\ominus}(NH_4OH,s)$. These quantities appear in Table IV.

Using the values in Table IV, along with our calculated enthalpy of formation, gives a true lattice potential energy (U^{true}_{POT}) of 842 kJ mol^{-1}, and $\Delta_{soln}H^{\ominus} = 6.3$ kJ mol^{-1}. A generalized empirical formula, such as Bartlett–Jenkins' relation,[33] is typically used when the formation enthalpy is unknown. It is instructive to use it here because we may estimate the hydrogen bond enthalpy in NH_4OH. This relation is derived from molecular volumes for nonhydrogen-bonded salts, and we would expect the lattice potential to be larger in hydrogen-bonded systems due to the additional bond energy. Indeed, large differences between U^{true}_{POT} and U_{POT}, as calculated from Eq. (2) for NH_4F and NH_4SH are attributable to hydrogen bonding. The lattice potential of MX (1:1) salts is given as

$$U_{POT} = 2I\left(\frac{\alpha}{\sqrt[3]{V}} + \beta\right)\ \mathrm{kJ\,mol^{-1}}, \quad (2)$$

where $\alpha = 117.3$ kJ mol^{-1} nm, $\beta = 51.9$ kJ mol^{-1}, and I is the ionic strength ($I = \Sigma n_k z_k^2$, where n_k is the number of ions of charge z_k in the formula unit).[33] V (nm^3) is, the volume per formula unit of the salt. Using the molecular volume for ammonium hydroxide calculated here (0.0529 nm^3) yields $U_{POT} = 729$ kJ mol^{-1}. This differs from U^{true}_{POT} by 113 kJ mol^{-1}. The structure of ammonium hydroxide is that of an NH_4^+ ion tetrahedrally coordinated, donating four hydrogen bonds to its nearest neighbor OH^- ions. The OH^- ions do-

TABLE IV. Thermodynamic data used to construct the Born–Fajans–Haber cycle for NH_4OH. All values are in units of kJ mol^{-1}.

$\Delta_f H^{\ominus}[NH_3(g)]$[a]	−45.94
$\Delta_f H^{\ominus}[H_2O(l)]$[a]	−285.83
$\Delta_{soln}H^{\ominus}[NH_3(g)]$[a]	−30.50
$\Delta_{hyd}H^{\ominus}[NH_4^+(g)] + \Delta_{hyd}H^{\ominus}[OH^-(g)]$[b]	−852.1

[a]Reference 48.
[b]Reference 49.

nate and receive one hydrogen bond to/from their neighboring anions as well as accepting four weaker hydrogen bonds from surrounding cations. Hence there are five hydrogen bonds per molecule, suggesting that the average hydrogen bond enthalpy in ammonium hydroxide is $\sim 113/5 \approx 22.6\,\mathrm{kJ\,mol^{-1}}$. The energy of the average hydrogen bond in AMH is $(1/5)\ [\Delta_f H^{\ominus}\mathrm{NH_3\cdot H_2O}, s - \{\Delta_f H^{\ominus}\mathrm{H_2O}, g + \Delta_f H^{\ominus}\mathrm{NH_3}, g\}] \approx 13.5\,\mathrm{kJ\,mol^{-1}}$. The increased electrostatic interactions in the ionic solid help to explain why the hydrogen bond in ammonium hydroxide is stronger.

V. SUMMARY

We have performed the first *ab initio* pseudopotential plane-wave calculations on the ambient pressure monohydrate of ammonia and found excellent agreement with the experimental structure and equation of state. Significant differences in the pressure dependence of covalent O–H and N–H bond lengths from ice VIII and solid ammonia are seen. Our simulated structure spontaneously transforms to an ionic solid (NH_4OH) at $\sim$5 GPa, which, in spite of similarities in the EOS, appears not to be related to the high-pressure phase IV of AMH. Nevertheless, NH_4OH could be stable at temperatures below 100 K. At a pressure of $\sim$35 GPa, another phase transition is observed, and this is currently under study.

We find that the enthalpy difference between AMH I, and ammonium hydroxide at zero Kelvin is $\sim 15\ \mathrm{kJ\,mol^{-1}}$, and this figure is used to derive an estimate of the heat of formation of ammonium hydroxide at 298 K of $-356\ \mathrm{kJ\,mol^{-1}}$. This value is consistent with current models describing the energy barrier to cation rotation, and the expected contribution of hydrogen bond enthalpy to the conventional electrostatic lattice enthalpy.

The implications for the other stoichiometric hydrates of ammonia are very significant. The potential exists for similar protolysis reactions to occur in ammonia dihydrate (ADH) and ammonia hemihydrate (AHH). Indeed, this may contribute to the breakdown of a possible ammonium hydroxide monohydrate ($NH_4OH\cdot H_2O$) into separate ammonium hydroxide and water ice phases in ADH. Moreover, comparison with the known alkali metal hydroxide hydrates shows that there may be considerable scope for additional stoichiometric, or nonstoichiometric, compounds ($NH_4OH\cdot nH_2O$) to occur at moderate pressures inside icy satellites. If it is the case that ADH also becomes ionic at moderate pressures, then there may be far reaching consequences for the geophysics of large icy bodies in our solar system. Work on the ambient pressure phases of ADH and AHH is currently in progress.

ACKNOWLEDGMENTS

One of the authors (A.D.F.) acknowledges a scholarship from the UCL graduate school in support of this work. The authors would like to acknowledge useful conversations with David Price.

[1] J. Loveday and R. J. Nelmes, in *Science and Technology of High Pressure: Proceedings of AIRAPT-17*, edited by M. H. Manghnani, W. J. Nellis, and M. T. Nicol (Universities Press, Hyderabad, India, 2000).
[2] D. A. Johnson, J. Chem. Soc. Dalton Trans. **1988**, 445 (1988).
[3] R. Prinn and B. Fegley, Astrophys. J. **249**, 308 (1981).
[4] J. S. Kargel, Icarus **100**, 556 (1992).
[5] J. I. Lunine, Y. L. Yung, and R. D. Lorenz, Planet. Space Sci. **47**, 1291 (1999).
[6] S. K. Croft, J. I. Lunine, and J. S. Kargel, Icarus **73**, 279 (1988).
[7] M. L. Johnson and M. Nicol, J. Geophys. Res., [Space Phys.] **92**, 6339 (1987).
[8] R. J. Nelmes, ISIS Experimental Report, RB 11246 (2000).
[9] A. D. Fortes, L. Vočadlo, J. P. Brodholt, and I. G. Wood (unpublished).
[10] A. D. Fortes, L. Vočadlo, J. P. Brodholt, and I. G. Wood (unpublished).
[11] R. J. Nelmes, ISIS Experimental Report, RB 9412 (1998).
[12] G. Brink and L. Glasser, J. Mol. Struct. **160**, 357 (1987).
[13] P. Hohenberg and W. Kohn, Phys. Rev. B **136**, B864 (1964); W. Kohn and L. J. Sham, *ibid.* **140**, A1133 (1965).
[14] J. P. Perdew and Y. Wang, Phys. Rev. B **45**, 13 (1992).
[15] D. R. Hamann, Phys. Rev. B **55**, 10 157 (1997).
[16] S. Tsuzuki and H. P. Lüthi, J. Chem. Phys. **114**, 3949 (2001).
[17] D. Vanderbilt, Phys. Rev. B **41**, 7892 (1990).
[18] G. Kresse and J. Furthmüller, Phys. Rev. B **54**, 11 (1996).
[19] H. J. Monkhorst and J. D. Pack, Phys. Rev. B **13**, 5188 (1976).
[20] W. S. Benedict, J. Chem. Phys. **24**, 1139 (1956).
[21] J. Demaison, L. Margulès, and J. E. Boggs, Chem. Phys. **260**, 65 (2000).
[22] S. B. Andrews, N. A. Burton, and I. H. Hillier, Chem. Phys. Lett. **280**, 73 (1997).
[23] S. Scheiner and M. Čuma, J. Am. Chem. Soc. **118**, 1511 (1996).
[24] T. Matsuo, A. Inaba, O. Yamamuro, and N. Onada-Yamamuro, J. Phys.: Condens. Matter **12**, 8595 (2000).
[25] F. Birch, J. Geophys. Res. **57**, 227 (1952).
[26] J.-P. Poirier and A. Tarantola, Phys. Earth Planet. Inter. **109**, 1 (1998).
[27] F. D. Murnaghan, Proc. Natl. Acad. Sci. USA **30**, 244 (1944).
[28] J. H. Rose, J. R. Smith, F. Guinea, and J. Ferrante, Phys. Rev. B **29**, 2963 (1984).
[29] S. K. Sikka, Phys. Rev. B **38**, 8463 (1988).
[30] J. Hafner, Acta Mater. **48**, 71 (2000).
[31] S. K. Croft, J. I. Lunine, and J. Kargel, Icarus **73**, 279 (1988).
[32] M. Fuchs, M. Bockstedte, E. Pehlke, and M. Scheffler, Phys. Rev. B **57**, 2134 (1998).
[33] H. D. B. Jenkins, H. K. Roobottom, J. Passmore, and L. Glasser, Inorg. Chem. **38**, 3609 (1999).
[34] L. Mercury, P. Vieillard, and Y. Tardy, Appl. Geochem. **16**, 161 (2001).
[35] F. Leclercq, P. Damay, and M. Foukani, J. Chem. Phys. **102**, 4400 (1995).
[36] J. E. Bertie and M. R. Shehata, J. Chem. Phys. **83**, 1449 (1985).
[37] J. M. Besson, Ph. Pruzan, S. Klotz *et al.*, Phys. Rev. B **49**, 12 540 (1994).
[38] L. Ojamäe, K. Hermansson, R. Dovesi, C. Roetti, and V. R. Saunders, J. Chem. Phys. **100**, 2128 (1994).
[39] P. A. Giguere, Rev. Chim. Miner. **20**, 588 (1983).
[40] T. Amano, J. Mol. Spectrosc. **103**, 436 (1984).
[41] R. J. C. Brown, J. Mol. Struct. **345**, 77 (1995).
[42] A. C. Lawson, R. B. Roof, J. D. Jorgensen, B. Morosin, and J. E. Schirber, Acta Crystallogr., Sect. B: Struct. Sci. **45**, 212 (1989).
[43] S. J. van Reeuwijk, K. G. van Beek, and D. Feil, J. Phys. Chem. A **104**, 10 901 (2000).
[44] M. Kh. Karapet'yants and M. L. Karapet'yants, *Thermodynamic Constants of Inorganic and Organic Compounds*, translated by J. Schmorak (Humphrey Scientific Publishers, Ann Arbor, MI, 1970).
[45] D. A. Johnson, Phys. Chem. Chem. Phys. **2**, 2903 (2000).
[46] D. L. Hildenbrand and W. F. Giaque, J. Am. Chem. Soc. **75**, 2811 (1953).
[47] A. Alavi, R. M. Lynden-Bell, and R. J. C. Brown, J. Chem. Phys. **110**, 5861 (1999).
[48] *CRC Handbook of Chemistry and Physics*, 81st ed., edited by David R. Lide (CRC, Boca Raton, FL, 2001).
[49] H. D. B. Jenkins, J. Solution Chem. **22**, 1029 (1993).